Published in final edited form as:
Biochemistry. 2007 June 19; 46(24): 7138–7145. doi:10.1021/bi602649u.

PLASMON WAVEGUIDE RESONANCE SPECTROSCOPIC EVIDENCE FOR DIFFERENTIAL BINDING OF OXIDIZED AND REDUCED *RHODOBACTER CAPSULATUS* CYTOCHROME C_2 TO THE CYTOCHROME BC_1 COMPLEX MEDIATED BY THE CONFORMATION OF THE RIESKE IRON-SULFUR PROTEIN†

S. Devanathan§, **Z. Salamon**§, **G. Tollin**§, **J. C. Fitch**§, **T. E. Meyer**§, **E. A. Berry**‡, and **M. A. Cusanovich**§,*

§*Department of Biochemistry and Molecular Biophysics, University of Arizona, Tucson AZ 85721*

‡*Physical Biosciences Division, Lawrence Berkeley National Laboratory, 1 Cyclotron Road, Berkeley, CA 94720*

Abstract

The dissociation constants for the binding of *Rhodobacter capsulatus* cytochrome c_2 and its K93P mutant to the cytochrome bc_1 complex embedded in a phospholipid bilayer were measured by plasmon waveguide resonance spectroscopy in the presence and absence of the inhibitor stigmatellin. The reduced form of cytochrome c_2 strongly binds to reduced cytochrome bc_1 (K_d = 0.02 μM), but binds much more weakly to the oxidized form (K_d = 3.1 μM). In contrast, oxidized cytochrome c_2 binds to oxidized cytochrome bc_1 in a biphasic fashion with K_d values of 0.11 μM and 0.58 μM. Such a biphasic interaction is consistent with binding to two separate sites or conformations of oxidized cytochrome c_2 and/or cytochrome bc_1. However, in the presence of stigmatellin, we find that oxidized cytochrome c_2 binds to oxidized cytochrome bc_1 in a monophasic fashion with high affinity (K_d = 0.06 μM) and reduced cytochrome c_2 binds less strongly (K_d = 0.11 μM) but ~30 fold more tightly than in the absence of stigmatellin. Structural studies with cytochrome bc_1, with and without the inhibitor stigmatellin, have lead to the proposal that the Rieske protein is mobile, moving between the cytochrome b and cytochrome c_1 components during turnover. In one conformation, the Rieske protein binds near the heme of cytochrome c_1, while the cytochrome c_2 binding site is also near the cytochrome c_1 heme but on the opposite side from the Rieske site, where cytochrome c_2 cannot directly interact with Rieske. However, the inhibitor, stigmatellin, freezes the Rieske protein iron-sulfur cluster in a conformation proximal to cytochrome b and distal to cytochrome c_1. We conclude from this that the dual conformation of the Rieske protein is primarily responsible for biphasic binding of oxidized cytochrome c_2 to cytochrome c_1. This optimizes turnover by maximizing binding of the substrate, oxidized cytochrome c_2, when the iron-sulfur cluster is proximal to cytochrome b and minimizing binding of the product, reduced cytochrome c_2, when it is proximal to cytochrome c_1.

Keywords

Stigmatellin; protein-protein interaction; binding constants; structural changes

†This work was supported by NIH grant GM (to M.A.C.)

*Corresponding author E-mail: cusanovi@u.arizona.edu Fax: 520 621 6603 Phone: 520 621 7533

In its simplest form, bacterial photosynthesis involves electron transfer between two membrane-bound complexes, the photosynthetic reaction center (RC) and cytochrome bc_1 (BC1), which is mediated by lipid-soluble quinone and by water-soluble cytochrome c_2 (C2). Upon absorption of light, the special pair bacteriochlorophyll becomes oxidized and the quinone (Q_B) reduced. The reaction center is rapidly reduced by C2 to complete the initial steps of the reaction. In the second half of the reaction, quinol is oxidized by the cytochrome b (B) and the Rieske iron-sulfur protein (ISP). The Rieske ISP transfers its electron to cytochrome c_1 (C1), which in turn reduces C2 to complete the cycle. During reduction of quinone, protons are taken up from the cytoplasmic side of the membrane; during subsequent oxidation of quinol, the protons are released on the periplasmic side, resulting in a proton gradient that is used to synthesize ATP. The three-dimensional structures of RC (1,2), BC1 (3-6), and C2 (7,8) have been determined. In addition, the crystal structures of the complexes of C2 and RC (9) and of cytochrome c (C) and BC1 (10) are known. Thus, the structures of all of the components of the pathway and their immediate interaction partners have been determined, but what is missing is the precise mechanism by which the electron transfer process is carried out and turnover optimized.

To date, considerable attention has been focused on the role of C2 in mediating electron transfer between reduced BC1 and the oxidized RC. Studies of the kinetics of electron transfer have emphasized the contribution of electrostatic interactions between negative charges on RC and positive charges on C2 to facilitate binding and electron transfer at low ionic strength. However, hydrophobic interactions and hydrogen bonding also contribute to binding. Thus, it has been proposed that electrostatics steer the C2 toward the optimum binding site on the RC, but that hydrophobic interactions then provide the primary stabilization of the bound complex (11, 12). Binding constants typically have been indirectly derived from kinetics of electron transfer (e.g. 13), although a few direct measurements have been performed (e.g. 14).

It is well established that C2, and more generally Class I c-type cytochromes, are substantially less stable in the oxidized state as compared to the reduced state due to the buried positive charge on the ferric heme iron. This differential stability is in part manifested by a dynamic conformational change that is present in only the oxidized cytochrome. This dynamic process involves the breakage of the methionyl sulfur-Fe^{+3} bond and the rapid movement ($\sim 30\ s^{-1}$) of the methionine (M96 in *Rb. capsulatus* C2) and adjacent amino acids ($\sim$ positions 90 – 100, the so-called “hinge region”) away from the heme face (15). We recently found, using plasmon waveguide resonance (PWR) spectroscopy, that dissociation of the oxidized C2 (C2 (ox)) – reduced RC complex is facilitated by the hinge movement (16). Key to these studies was the use of the C2 mutant K93P which has hinge kinetics that are ~25 fold faster than in the wild-type cytochrome ($\sim 700\ s^{-1}$) and 30-fold weaker binding to RC. In the case of RCs, reduced wild-type C2 binds to both a high- and low-affinity site, while wild-type C2 (ox) and both redox states of the mutant C2 can only bind to the low-affinity site. This was attributed to the more stable structure of reduced wild-type C2 and to a conformational change occurring upon oxidation of C2, which occurs more readily in the oxidized K93P mutant, resulting in a form incapable of high-affinity binding (16).

There have been a number of studies on the interaction of cytochromes (C or C2) with BC1 (reviewed by Millett & Durham, 17). There are strong parallels with the RC studies in that the C2/BC1 interaction has a large electrostatic component that steers the reactants for optimum binding, which is primarily hydrophobic in nature. In the yeast system, intracomplex electron transfer from the Rieske ISP to C1 occurs with a rate constant of $\sim 80{,}000\ s^{-1}$, although the overall reaction is gated by movement of the Rieske ISP between the B and C1 centers (17). Within the preformed complex of C and BC1 at low ionic strength, electron transfer from C1 to C also is very fast, occurring with a rate constant of $\sim 14{,}000\ s^{-1}$, with an apparent μM dissociation constant (18). One might expect a similar mechanism for substrate binding and

product release as with RC, i.e. a dynamic conformational change that facilitates product release and thus turnover. The products in the case of reaction with BC1 are reduced C2 (C2 (red)) and oxidized C1 (C1 (ox)), with C2 (red) being a relatively stable structure with no "hinge" movement. However, both C1 and C2 are class I cytochromes that share a common fold. Thus, it is possible that C1 (ox) undergoes a dynamic conformational change to facilitate product release. Note however, that the situation with BC1 is somewhat more complex than RC as the Rieske ISP has been shown to be mobile and can be found proximal to both the B and to the C1 depending on conditions (4). Movement of the Rieske ISP has been very well documented in several species and is an integral part of the mechanism (19-23). Indeed, in the presence of the BC1 inhibitor stigmatellin, the Rieske ISP associates with the B cytochrome and the iron-sulfur cluster is distal from C1 in the BC1 complex. In what follows, we report PWR studies on the interaction of *Rhodobacter capsulatus* C2 (oxidized and reduced) with BC1 in a phospholipid bilayer, using wild-type and mutant C2 (K93P) and the inhibitor stigmatellin.

MATERIALS & METHODS

Rhodobacter capsulatus cytochrome BC1 complex was prepared from 100 g MT-G4/S4 membranes following the protocol of Andrews et al (24) for *Rb. sphaeroides*, except that 1.5 mg dodecylmaltoside per mg protein (Anatrace, Maumee, OH) was used (25). High purity glycerol (ICN, Aurora OH) was used in the initial extraction and purification steps, and 1% SDS was used in the BCA protein assay (Pierce) used to measure total membrane protein concentration. The enzymatic activity of dodecylmaltoside solubilized BC1 was measured to establish that it was functional with turnover numbers in the range reported in the absence of phospholipid (24). Prior to incorporation of purified BC1 into the lipid bilayer, it was dialyzed against 30 mM octylglucoside (Sigma), 10 mM Tris-Cl, 100 mM KCl, 1 mM EDTA, pH 7.3. Wild-type C2 and mutant K93P were prepared as described by Dumortier et al (15). For PWR experiments, C2 was oxidized with ferricyanide prior to dialysis, and C2 and BC1 were reduced with an excess of sodium dithionite (prior to dialysis in the case of C2). The C2 was dialyzed against the reaction buffer, 100 mM KCl, 10 mM Tris-Cl, pH 7.3.

Self-assembled lipid bilayers were formed using a solution of 8 mg/mL egg phosphatidyl-choline (Avanti Polar Lipids, Birmingham AL) in butanol/squalene (10:0.1 v/v). A small amount of lipid solution (1.5 μl) was injected into the orifice in a Teflon block separating the silica surface of the PWR resonator from the aqueous phase as previously described (16). Spontaneous bilayer formation was initiated when the sample compartment was filled with aqueous buffer solution. The BC1 complex was inserted into the lipid bilayer (~ 5.5 nm thickness by 3 mm diameter) by addition of BC1 (50 μM stock, final concentration ~10 nM) in detergent-containing buffer to the aqueous compartment of the PWR cell (volume, 0.5 ml). This results in dilution of the detergent below the critical micelle concentration and to spontaneous transfer of the protein from the detergent micelle into the lipid membrane. The bilayer containing BC1 was washed with the reaction buffer to remove detergent and excess BC1 prior to measurement, and titrated with C2 or K93P (16,26). Based on prior studies (27) the amount of BC1 in the bilayer was on the order of 400 femtomoles (oriented in both directions) and the C2 amounts in the cell ranging from 500 femtomoles to 50 nmoles depending on the experiment. As shown previously, C2 does not bind to the phosphatidyl-choline bilayer in the absence of BC1 at the concentrations of C2 used here (16). For stigmatellin experiments, the BC1-containing bilayer was titrated with 100 μM stigmatellin (Fluka) in ethanol to saturation, prior to titration with C2. The principles of PWR spectroscopy have been extensively described previously (16,28,29). Experiments were performed with 543 nm laser illumination using a beta PWR instrument from Proterion Corp. (Piscataway NJ) with an angular spectral resolution of 1 mdeg.

For modeling, C1 and the Rieske ISP structures in the "B" position are from a refined version of the *Rb. capsulatus* structure 1ZRT (6, RCSB Protein Data Bank), incorporating some corrections based on the higher-resolution structure of *Rb. sphaeroides* BC1 complex 2FYN (30). The ISP in the "C1" position is also from this structure, repositioned as in the bovine BC1 structure 1BE3 (31) as described below. The C2 structure is *Rb. capsulatus* 1C2R (7), positioned as in the yeast BC1 structure 1KYO (10). The three BC1 structures (1ZRT, 1BE3, and 1KYO) were superimposed based on the cytochrome b dimer. To obtain the ISP in the "C1" position, the ISP chains from 1ZRT were superimposed on the ISP chains of thus-positioned 1BE3. Likewise, the C2 structure 1C2R was superimposed on yeast C in thus-positioned 1KYO.

RESULTS

Upon incorporation of the BC1 complex into the lipid bilayer, the PWR spectra showed shifts in resonance position toward higher angles of incidence, as well as changes in amplitude, for both *p*- and *s*-polarization, as expected for successful insertion of protein into the bilayer (data not shown; cf. 16). Addition of aliquots of either reduced or oxidized C2 to BC1 (ox) resulted in significant changes in the PWR spectra as shown in Figure 1, where the spectral shift is plotted against the concentration of C2 in the sample compartment. Because the amount of BC1 incorporated is generally much smaller than the amount of C2 added, ligand binding does not significantly deplete the C2 concentration. The binding of C2 (red) to BC1 (ox) (Figure 1A) resulted in shifts to lower incident angle, with much larger effects for *p*- than for *s*-polarization. Such negative shifts in both polarizations reflect a decrease in proteolipid bilayer mass that are consistent with a change in protein conformation that results in an increase in the volume that the BC1 occupies within the bilayer and a consequent net transfer of lipid molecules into the lipid solution that anchors the bilayer to the Teflon spacer (Gibbs border). This decreases the total mass density in the bilayer. This type of behavior has been observed in a number of systems (for example 32) and is thought to reflect changes in the tilting of the transmembrane helices with respect to the plane of the membrane on ligand binding (33). Note that the magnitude of the PWR spectral shift increases as the C2 concentration increases. This allows a direct determination of the binding constant. The data were fit with hyperbolic functions (solid curves in Figure 1A) to obtain the dissociation constant, $K_d = 3.1 \pm 0.3$ μM (average of both polarizations). Note that the redox potential of *Rb. capsulatus* C1 is reported to be 320 mV in isolated BC1 complexes (0.01% dodecyl maltoside, 34) and that of *Rb. capsulatus* C2, 368 mV (35). Thus, for the BC1 (ox) titration with C2 (red) a mixture of redox complexes (BC1 (ox) – C2 (red) and BC1 (red) – C2 (ox) could be expected. However, we obtained a single hyperbolic curve (Figure 1A) with K_D quite distinct from those for the BC1 (red) – C2 (red) and BC1 (ox) – C2 (ox) complexes (see below). This could result from either of two factors. First, the C1 redox potential in the phospholipid bilayer could be significantly lower (for example, 30-40 mV) than in the isolated complex, which would reduce the amount of a BC1 (red)- C2 (ox) complex below the detectable limit of PWR. Note, this is in contrast to the report of Engstrom et al (18) who conclude the redox potentials of cytochrome c and BC1 were approximately the same using detergent solubilized yeast BC1 and kinetic analysis. The second possibility, that the binding constants for BC1 (ox) – C2 (red) and BC1 (red)- C2 (ox) complexes are similar is unlikely because of the results we observe in additional experiments described below.

In sharp contrast to the binding of C2 (red) to BC1 (ox), the binding of C2 (ox) to BC1 (ox) was biphasic, resulting in an initial increase in incident angle (as expected for an increase in total mass density) followed by a decrease (lower total mass density, again due to expulsion of lipid from the bilayer consequent to a protein conformation change) shown in Figure 1B. To fit the data, we used two hyperbolic functions of opposite sign, resulting in K_d values of 0.11 ± 0.01 μM and 0.58 ± 0.01 μM. These results are consistent with binding involving either

two separate sites on C2, or involving two different conformations of either BC1 or C2. We will return to this issue below.

In contrast to these results, the effect of adding C2 (red) to BC1 (red) on the PWR spectra (Figure 2) was a large increase in incident angles for both polarizations, with much stronger binding ($K_d = 0.02 \pm 0.003$ μM). This is consistent with binding of the C2 to the BC1 producing a net increase in total mass density in the membrane. Thus, if a conformational change occurred as a consequence of this binding event, it was much different from the change occurring upon binding to the BC1 (ox). Because of electron transfer, it is not possible to measure the binding of C2 (ox) to BC1 (red).

In the case of the binding of C2 (ox) to reduced RC, the mutant K93P had a significant effect, presumably due to the hinge dynamics as discussed above (16). Thus, we measured the binding of oxidized and reduced K93P to BC1. The expectation was that since there is no hinge movement in reduced K93P, it would have a binding constant similar to that of reduced wild-type C2. The results are shown in Figure 3B, where the fitted data gave a K_d of 0.023 ± 0.002 μM, which is identical to wild-type under the same conditions (see Figure 2). However, the binding of K93P (ox) with BC1 (ox) (shown in Figure 3A) was also similar to wild-type (compare **Figures** 1B **and** 3A), although binding in the initial phase was somewhat stronger (by a factor of two), and binding in the second phase produced a considerably less negative spectral shift but occurred with about the same affinity, yielding K_d values of 0.05 ± 0.002 μM and 0.63 ± 0.02 μM respectively. Thus, in sharp contrast to RC, the K93P mutation and corresponding change in the conformational equilibrium had only a minimal effect on binding to BC1 in either C2 redox state.

Because C2 hinge dynamics appear not to be as important in the BC1 system as in RC, we considered the possibility that multiple conformations of BC1 (ox) might be responsible for the biphasic binding of C2 (ox), particularly since the binding symmetry was reversed relative to RC-C2 binding, i.e. in the RC case, the high affinity binding event produced a negative spectral shift and the lower affinity binding produced a positive shift. Since structural studies have established that the Rieske ISP is mobile within the BC1 complex, and that the inhibitor stigmatellin positions the Rieske ISP proximal to the B and distal to C1 (4), we determined the effect of stigmatellin on C2 binding by BC1. As shown in Figure 4A, there was a dramatic change in binding of C2 (ox) with BC1 (ox) in the presence of stigmatellin, which showed single site binding (with $K_d = 0.06 \pm 0.01$ μM) coupled to a total mass increase, similar to the strong binding site ($K_d = 0.11$ μM) observed in the absence of inhibitor (compare with Figure 1B). Strikingly, the affinity of C2 (red) for BC1 (ox) (Figure 4B), was ~ 30 fold stronger in the presence of stigmatellin (see Figure 1A), although it was still half that of the C2 (ox). Note that the binding was coupled to an increase in total mass density, the opposite of what was observed in the absence of stigmatellin (compare with Figure 1A). Thus, we conclude that the biphasic binding of C2 (ox) to BC1 (ox) is due to the two locations of the Rieske ISP in the uninhibited protein. This will be discussed below.

DISCUSSION

PWR spectroscopy not only provides a powerful means to measure binding constants for membrane proteins and their ligands, but it is also capable of detecting changes in proteolipid membrane structure that take place upon binding. Table 1 summarizes the binding constants obtained in the studies with BC1 reported here, as well as the impact on membrane mass density. Interestingly, we find that the binding symmetry for C2 and BC1 was opposite to that for C2 and RC (16). Thus, C2 (ox) bound to BC1 (ox) in a biphasic manner consistent with two binding sites or conformations, the first site with an increase in net mass density and the second, lower affinity site, with a decrease in total mass density. In contrast, C2 (ox) bound to

a single RC site with a K_d of 10 nM, and with a net increase in total mass density. On the other hand, C2 (red) bound to a single BC1 (ox) site, although with much lower affinity than the oxidized cytochrome (Table 1), and resulted in a mass decrease. However, C2 (red) binding with RC was biphasic, with K_d values of 0.01 μM and 0.15 μM (16). Furthermore, in the RC case, binding at the high affinity site resulted in a decrease in net mass density, but this effect was reversed at the low affinity site. Note that for BC1, C2 (ox) is the substrate, as opposed to the reduced form which is the product, and would be expected to bind more strongly than the product, whereas with RC it is C2 (red) that is the substrate.

In the RC/C2 study (16), we investigated the possibility that C2 can exist in more than one conformation, and we found support for this argument using the K93P C2 mutant. This mutant bound monophasically to the RC in both oxidation states. However, in the case of BC1, we find that K93P (ox) bound biphasically with similar affinities to the wild type, and that the binding of K93P (red) was also similar to that of the wild type. Thus, we conclude that although an alternate conformation of C2 may have a significant role in the RC system, this was not the case with BC1.

If conformational changes in C2 have little or no effect on binding, then we have to consider the possibility that the biphasic binding is due to the BC1 structure, especially considering the large effect of stigmatellin. It is known from the crystal structure of BC1 complexes that conformational changes occur during its function, but it is the Rieske ISP that undergoes the largest movement during electron transfer (3-5), first picking up an electron from quinol at the Qo site in B, moving to a position near C1, and transferring the electron. The C1 subunit, to which C2 binds, appears to be relatively fixed in orientation; and to a first approximation it is difficult to imagine how the position of the ISP subunit might affect the binding of C2. Figure 5a presents a hypothetical model of the structure of the *Rb. capsulatus* C2/C1/ISP complex (see the Materials and Methods for the details of the modeling) in the presence of stigmatellin, with the Rieske iron-sulfur center close to the B subunit (“B” position). Figure 5b presents the same view with the iron-sulfur center near the C1 (“C1” position), presumably in the absence of inhibitor a mixture of the “B” and “C1” positions is present. As shown in the present experiments (see Table 1), stigmatellin, and thus the position of the ISP has a strong effect on the binding of C2 to C1. Thus, C2 (ox) binding with BC1 (ox) titrates as a single site in the presence of stigmatellin with a binding constant similar to that of the high affinity site in the absence of stigmatellin, with an increase in total mass density in both cases. We conclude that the biphasic binding of C2 (ox) by BC1 (ox) in the absence of stigmatellin is due to the two conformations of ISP, resulting in tight binding when ISP is adjacent to B and lower affinity binding when it is near C1. Presumably, during electron transfer, the ISP and quinol bind to the B site, with C2 (ox) binding to C1 (ox) with high affinity (~100 nM). Following electron transfer from quinol to ISP and dissociation of the quinone, the reduced Rieske swings to its C1 interaction site, rapidly transfers an electron to the C1 (~80,000 s^{-1}) which then reduces the bound C2 (~14,000 s^{-1}) with the C1 (ox)-C2 (red) complex having low affinity (~3 μM), thus releasing the C2 and facilitating turnover. In this scheme, the low affinity site for C2 (ox) on C1 (ox) is a consequence of the alternate C1 conformation within the ternary complex with oxidized ISP, but not directly relevant to electron transfer *per se*.

Given that stigmatellin binding and its influence on the orientation of the Rieske ISP affect the binding of C2, it follows that the ISP-C1 and C1-C2 interaction domains must communicate. Figure 6 presents a close-up stereo view of the C2-C1 and ISP-C1 interaction interfaces. Figure 6A is a ribbon representation and illustrates the relationship of the polypeptides of C1, C2 and Rieske ISP. Note that there are extensive interactions between C1 and both the C2 and Rieske ISP, but no direct interaction between C2 and the ISP. However, it is clear, at least in the model, that Y152 and Y153 in C1 bridge the electron donor and acceptor, with Y152 approaching the C2 heme and Y153 directed towards the Rieske iron-sulfur cluster (Figure 6B). This opens the

possibility that when the ISP binds to C1, a conformational change is propagated through the tyrosine bridge resulting in alteration of the C2/C1 interaction domain and *vice versa*. Thus, we envision a push-pull mechanism whereby the Rieske ISP can exert an effect on C2 binding.

Based on the RC-C2 studies, where C2 hinge dynamics clearly modulate binding, we expected that the C2 (ox) – C1 (ox) binding would be weak relative to the reduced-reduced or oxidized-reduced interactions. This would be particularly true if both oxidized C1 and C2 had dynamic properties at the site of interaction which facilitated turnover. This appears to be the case when comparing oxidized-oxidized (0.110 and 0.580 μM) and reduced-reduced (0.020 μM) affinities, consistent with some role for hinge dynamics in this system. Moreover, the very weak apparent affinity of C2 (red) for C1 (ox) supports the view that product release, hence turnover, is facilitated by structural changes resulting from reducing one or both reactants. However, the magnitude of the decrease in affinity of BC1 (ox) for C2 (red) was surprising suggesting that additional factors (distinct from hinge dynamics) are involved. Interestingly, the low affinity site for C2 (ox) and binding of C2 (red) to BC1 (ox) both involve a decrease in total membrane mass density, suggesting that binding drives a structural change which alters the alignment of the transmembrane helices contributed by all three subunits to produce a structure that occupies a larger bilayer volume, thereby forcing lipid into the Gibbs border that anchors the bilayer to the resonator surface. In contrast, binding C2 (ox) at the high affinity BC1 site (both wild-type C2 and K93P) with and without stigmatellin, and the binding of C2 (red) to BC1 (ox) with stigmatellin, all involve an increase in mass density. These results are consistent with a model in which the high affinity site is present when the Rieske protein is proximal to the B, and the low affinity site is present when the Rieske ISP is proximal to the C1. It follows then that binding C2 (red) to BC1 (ox) generates a structure where the Rieske ISP is proximal to the C1 and that stigmatellin reverses this effect.

Note that we cannot measure the binding of C2 (ox) (the substrate) to BC1 (red) since the thermodynamics substantially favor C2 (red), and thus we can only speculate as to what this binding might be like. Biologically, it would make sense for C1 (red) to have a high affinity for C2 (ox), the substrate, and a low affinity for the Rieske ISP. That is, the Rieske ISP would be proximal to B after C1 is reduced, in preparation to be itself reduced, and thus to initiate the next cycle of electron transfer following C2 reduction.

There are several studies that report an approximation of binding constants for BC1 complexes and cytochromes c, generally obtained from steady state kinetics of detergent solubilized BC1 complex at various ionic strengths that represent the BC1 (red), C2 (ox) couple. For *Rb. sphaeroides*, a K_m of ~ 1 μM (36), for *Rb. capsulatus*, a K_m of ~ 3 μM (37), and bovine a K_m of ~ 1 μM (38) was obtained. A K_d derived from transient kinetics for yeast BC1 and cytochrome c interaction was ~ 1 μM (presumably for BC1(red) and C2(ox) at 110 mM ionic strength, see reference 18), although this was not determined from a titration. Of the four binding constants that describe the BC1-cytochrome c interaction, BC1 (red)-C2 (ox) binding was the only one we were unable to measure in equilibrium titrations. Of those binding constants which we could measure, that for BC1 (ox)-C2 (red) was most similar to those reported for the BC1(red)-cytochrome c (ox) interaction (~ 3 μM). It is surprising to us that the BC1(ox)-C2(ox) and BC1(red)-C2(red) binding constants were much stronger, but we have no direct comparison to previous work to judge the significance. Clearly, this needs to be investigated in future studies.

In summary, the two C2 redox states bind differentially to oxidized BC1. Importantly, stigmatellin and, as a consequence, the position of the Rieske ISP relative to B and C1, influence the C1-C2 interaction. Based on modeling, we propose that C1 side chains, at positions 152 and 153, bridge between the C2 and Rieske ISP interaction domains on C1, and modulate C2 binding.

Abbreviations

PWR, Plasmon Waveguide Resonance; K93P, mutation of cytochrome c_2 lysine 93 to proline; RC, photosynthetic reaction center; BC1, cytochrome bc_1 complex; C2, cytochrome c_2; ISP, Rieske iron-sulfur protein; Q, quinone.

REFERENCES

1. Deisenhofer J, Epp O, Miki K, Huber R, Michel H. Structure of the protein subunits in the photosynthetic reaction center of *Rhodopseudomonas viridis* at 3 A resolution. Nature 1985;318:618–624.
2. Allen JP, Feher G, Yeates TO, Komiya H, Rees DC. structure of the reaction center from *Rhodobacter sphaeroides* R-26: Protein-cofactor (quinones and Fe^{2+}) interactions. Proc. Natl. Acad. Sci. USA 1988;85:8487–8491. [PubMed: 3054889]
3. Xia D, Yu CA, Kim H, Xia JZ, Kachurin AM, Zhang L, Yu L, Deisenhofer J. Crystal structure of the cytochrome bc_1 complex from bovine heart mitochondria. Science 1997;277:60–66. [PubMed: 9204897]
4. Zhang Z, Huang LS, Shulmeister VM, Chi YI, Kim KK, Hung LW, Crofts AR, Berry EA, Kim SH. Electron transfer by domain movement in cytochrome bc_1. Nature 1998;392:677–684. [PubMed: 9565029]
5. Crofts AR, Guergova-Kuras M, Huang LS, Kuras R, Zhang Z, Berry EA. Mechanism of ubiquinol oxidation by the bc_1 complex: Role of the iron sulfur protein and its mobility. Biochemistry 1999;38:15791–15806. [PubMed: 10625445]
6. Berry EA, Huang LS, Saechao LK, Pon NG, Valkova-Valchanova M, Daldal F. X-ray structure of *Rhodobacter capsulatus* cytochrome bc1: Comparison with its mitochondrial and chloroplast counterparts. Photosynthesis Res 2004;81:251–275.
7. Benning MM, Wesenberg G, Caffrey MS, Bartsch RG, Meyer TE, Cusanovich MA, Rayment I, Holden HM. Molecular structure of cytochrome c_2 isolated from *Rhodobacter capsulatus* determined at 2.5 A resolution. J. Mol. Biol 1991;220:673–685. [PubMed: 1651396]
8. Axelrod HL, Feher G, Allen JP, Chirino AJ, Day MW, Hsu BT, Rees DC. Crystallization and X-ray structure determination of cytochrome c_2 from *Rhodobacter sphaeroides* in three crystal forms. Acta crystallogr 1994;D50:596–602.
9. Axelrod HL, Abresch EC, Okamura MY, Yeh AP, Rees DC, Feher G. X-ray structure determination of the cytochrome c_2: reaction center electron transfer complex from *Rhodobacter sphaeroides*. J Mol Biol 2002;319:501–15. [PubMed: 12051924]
10. Lange C, Hunte C. Crystal structure of the yeast cytochrome bc_1 complex with its bound substrate cytochrome c. Proc. Natl. Acad. Sci. USA 2002;99:2800–2805. [PubMed: 11880631]
11. Tetreault M, Cusanovich MA, Meyer TE, Axelrod H, Okamura MY. Double mutant studies identify electrostatic interactions that are important for docking cytochrome c_2 onto the bacterial reaction center. Biochemistry 2002;41:5807–5815. [PubMed: 11980484]
12. Gong XM, Paddock ML, Okamura MY. Interactions between cytochrome c_2 and photosynthetic reaction center from *Rhodobacter sphaeroides*: changes in binding affinity and electron transfer rate due to mutation of interfacial hydrophobic residues are strongly correlated. Biochemistry 2003;42:14492–14500. [PubMed: 14661961]
13. Tetreault M, Rongey SH, Feher G, Okamura MY. Interaction between cytochrome c_2 and the photosynthetic reaction center from *Rhodobacter sphaeroides*: effects of charge modifying mutations on binding and electron transfer. Biochemistry 2001;40:8452–8462. [PubMed: 11456482]
14. Rosen D, Okamura MY, Feher G. Interaction of cytochrome c with reaction centers of *Rhodopseudomonas sphaeroides* R-26: determination of number of binding sites and dissociation constants by equilibrium dialysis. Biochemistry 1980;19:5687–5692. [PubMed: 6257286]
15. Dumortier C, Remaut H, Fitch JC, Meyer TE, Van Beeumen JJ, Cusanovich MA. Protein dynamics in the region of the sixth ligand methionine revealed by studies of imidazole binding to *Rhodobacter capsulatus* cytochrome c_2 hinge mutants. Biochemistry 2004;43:7717–7724. [PubMed: 15196014]

16. Devanathan S, Salamon Z, Tollin G, Fitch JC, Meyer TE, Cusanovich MA. Binding of oxidized and reduced cytochrome c_2 to photosynthetic reaction centers: Plasmon waveguide resonance spectroscopy. Biochemistry 2004;43:16405–16415. [PubMed: 15610035]

17. Millett F, Durham B. Kinetics of electron transfer within cytochrome bc_1 and between cytochrome bc_1 and cytochrome c. Photosynthesis Res 2004;82:1–16.

18. Engstrom G, Rajagukguk R, Saunders AJ, Patel CN, Rajagukguk S, Merbitz-Zahradnik T, Xiao K, Pielak GJ, Trumpower B, Yu CA, Yu L, Durham B, Millett F. Design of a ruthenium-labeled cytochrome c derivative to study electron transfer with the cytochrome bc_1 complex. Biochemistry 2003;42:2816–2824. [PubMed: 12627947]

19. Darrouzet E, Valkova-Valchanova M, Moser CC, Dutton PL, Daldal F. Uncovering the [2Fe2S] domain movement in cytochrome BC1 and its implications for energy conversion. Proc. Natl. Acad. Sci. USA 2000;97:4567–72. [PubMed: 10781061]

20. Valkova-Valchonova M, Darrouzet E, Moomaw CR, Slaughter CA, Daldal F. Proteolytic cleavage of the Fe-S subunit hinge region of Rhodobacter capsulatus BC1 complex: Effects of inhibitors and mutation. Biochemistry 2000;39:15484–92. [PubMed: 11112534]

21. Xiao K, Yu L, Yu CA. Confirmation of the involvement of protein domain movement during the catalytic cycle of the cytochrome BC1 complex by the formation of an intersubunit disulfide bond between cytochrome B and the iron-sulfur protein. J. Biol. Chem 2000;275:38592–604.

22. Bowman MK, Berry EA, Roberts EA, Kramer DM. Orientation of the g-tensor axes of the Rieske subunit in the cytochrome BC1 complex. Biochemistry 2004;43:430–6. [PubMed: 14717597]

23. Covian R, Trumpower BL. Regulatory interaction between ubiquinol oxidation and ubiquinone reduction sites in the dimeric cytochrome BC1 complex. J. Biol. Chem 2006;281:30925–32. [PubMed: 16908520]

24. Andrews KM, Crofts AR, Gennis RB. Large-Scale Purification and characterization of a Highly Active Four-Subunit Cytochrome BC1 Complex From *Rhodobacter sphaeroides*. Biochem 1990;29:2645–51. [PubMed: 2161250]

25. Ljungdahl PO, Pennoyer JD, Robertson DE, Trumpower BL. Purification of Highly Active Cytochrome BC1 Complexes From Phylogenetically Diverse Species by a Single Chromatographic Procedure. Biochim. Biophys. Acta 1987;891:227–241. [PubMed: 3032252]

26. Salamon Z, Brown MF, Tollin G. Plasmon resonance spectroscopy: probing interactions within membranes. Trends Biochem. Sci 1999;24:213–219. [PubMed: 10366845]

27. Salamon Z, Tollin G. Surface Plasmon Resonance Studies of Complex Formation Between Cytochrome c and Bovine Cytochrome c Oxidase Incorporated into a Supported Planar Lipid Bilayer. II. Binding of Cytochrome c to Oxidase Containing Cardiolipin/Phosphatidylcholine Membranes. Biophysical J 1996;71:858–867.

28. Salamon Z, Macleod HA, Tollin G. Coupled plasmon-waveguide resonators: a new spectroscopic tool for probing proteolipid film structure and properties. Biophys. J 1997;73:2791–2797. [PubMed: 9370473]

29. Salamon Z, Tollin G. Plasmon resonance spectroscopy: probing molecular interactions at surfaces and interfaces. Spectroscopy 2001;15:161–175.

30. Esser L, Gong X, Yang S, Yu L, Yu CA, Xia D. Surface-modulated motion switch: capture and release of iron-sulfur protein in the cytochrome BC1 complex. Proc. Natl. Acad. Sci. USA 2006;103:13045–50. [PubMed: 16924113]

31. Iwata S, Lee JW, Okada K, Lee JK, Iwata M, Rasmussen B, Link TA, Ramaswamy S, Jap BK. Complete structure of the 11-subunit bovine mitochondrial cytochrome BC1 complex. Science 1998;281:64–71. [PubMed: 9651245]

32. Alves ID, Cowell SM, Salamon Z, Devanathan S, Tollin G, Hruby VJ. Different structural states of the proteolipid membrane are produced by ligand binding to the human delta opioid receptor as shown by plasmon-waveguide resonance spectroscopy. Mol. Pharmacol 2004;65:1248–1257. [PubMed: 15102953]

33. Salamon Z, Cowell S, Varga E, Yamamura HI, Hruby VJ, Tollin G. Plasmon resonance studies of agonist/antagonist binding to the human delta-opioid receptor: new structural insights into receptor-ligand interactions. Biophys. J 2000;79:2463–2474. [PubMed: 11053123]

34. Osyczka A, Dutton PL, Moser CC, Darrouzet E, Daldal F. Controlling the Functionality of Cytochrome c_1 Redox Potentials in the *Rhodobacter capsulatus* bc_1 Complex through Disulfide Anchoring of a Loop and β-Branched Amino Acid near the Heme-Ligating Methionine. Biochemistry 2001;40:14547–14556. [PubMed: 11724568]

35. Pettigrew GW, Meyer TE, Bartsch RG, Kamen MD. pH Dependence of the Oxidation Reduction Potential of Cytochrome c_2. Biochim. Biophy. Acta 1975;430:197–208.

36. Gabellini N, Bowyer JR, Hurt E, Melandri BA, Hauska G. A Cytochrome b/c_1 Complex With Ubiquinol - Cytochrome C_2 Oxidoreductase Activity From *Rhodopseudomonas sphaeroides* GA. Eur. J. Biochem 1982;126:105–111. [PubMed: 6290210]

37. Güner S, Willie A, Millett F, Caffrey MS, Cusanovich MA, Robertson DE, Knaff DB. The Interaction Between Cytochrome C_2 and The Cytochrome bc_1 Complex in The Photosynthetic Purple Bacteria *Rhodobacter capsulatus* and *Rhodopseudomonas viridis*. Biochem 1993;32:4793–4800. [PubMed: 8387815]

38. Kubota T, Yoshikawa S, Matsubara H. Kinetic Mechanism of Beef Heart Ubiquinol: Cytochrome c Oxidoreductase. J. Biochem 1992;111:91–98. [PubMed: 1318882]

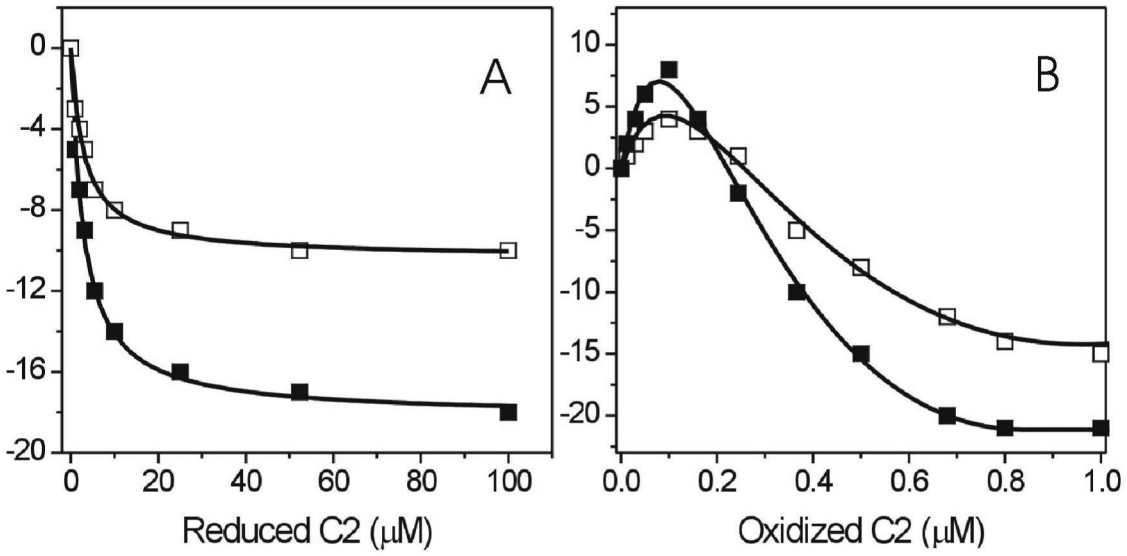

Figure 1.

Wild-type C2 binding to bilayer-incorporated oxidized BC1: plots of PWR spectral minimum as a function of concentration of wild-type C2. A. Titration of oxidized BC1 with reduced C2, where the solid line shows the fit to the experimental data with a single hyperbolic function. Negative values are indicative of resonance shifts to smaller incident angles. B. Titration of oxidized BC1 with oxidized C2, where solid lines are fits with two hyperbolic curves of opposite sign. Buffer, in the sample compartment is 10 mM Tris, 100 mM KCl, pH 7.3, 25 ° C. Filled squares, p-polarization, open squares s-polarization. Dissociation constants (K_d) values from hyperbolic fits are reported in Table 1. The estimated error in resonance angle position in these experiments is ± 1 mdeg.

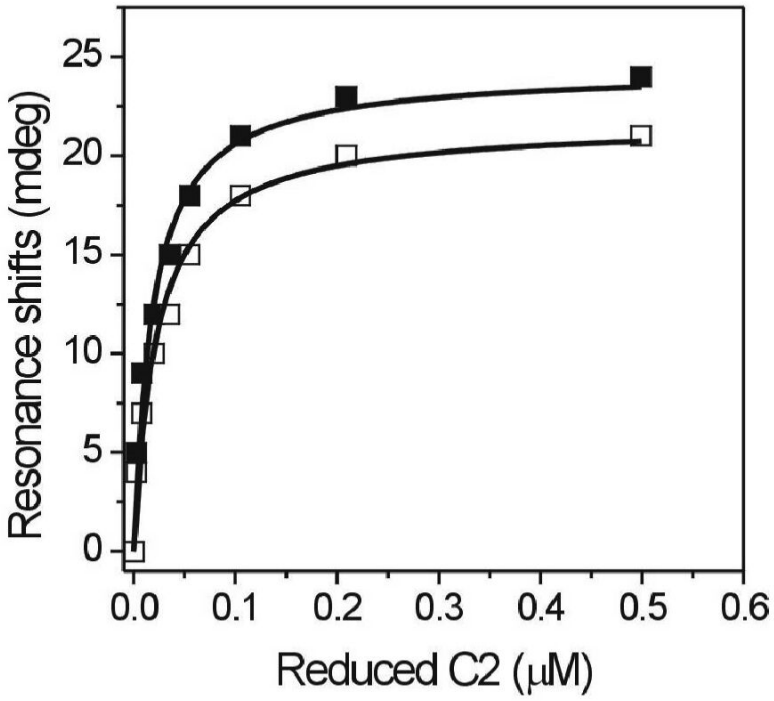

Figure 2.
Binding of reduced wild-type C2 to bilayer-incorporated reduced BC1, PWR spectral resonance minimum shifts as a function of increasing reduced C2 concentration.. Conditions as in Figure 1, solid lines, fits with a single hyperbolic function. Filled squares, p-polarization, open squares, s-polarization. (K_d values reported in Table 1).

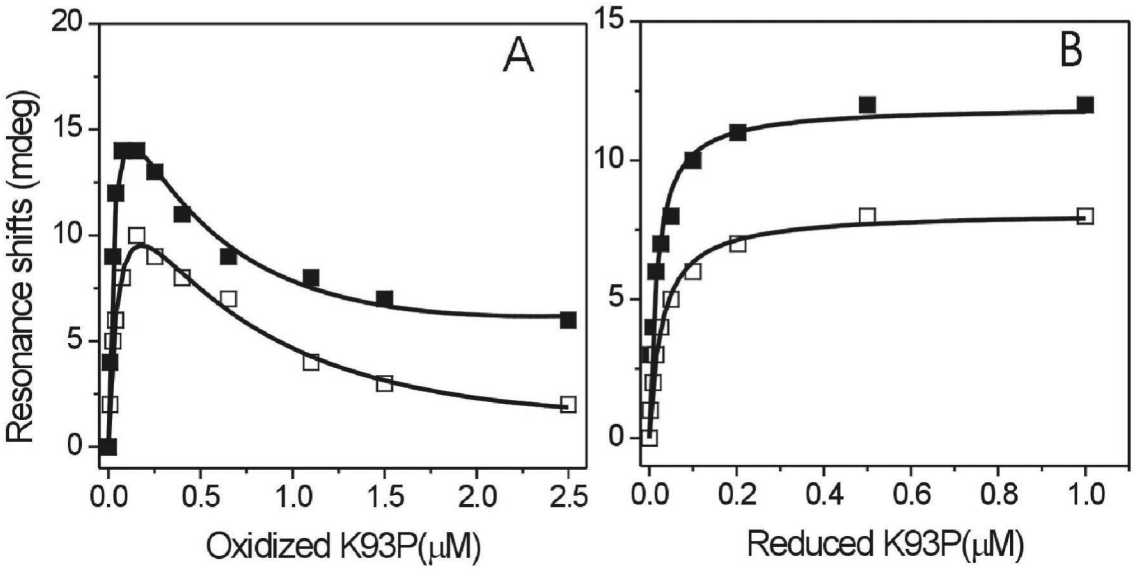

Figure 3.
K93P binding to BC1. A. Titration of oxidized bilayer-incorporated BC1 with oxidized K93P, solid lines, fits with two hyperbolic curves of opposite sign. B. Titration of reduced bilayer-incorporated BC1 with reduced C2, solid line, fit with a single hyperbola. Conditions as in Figure 1.

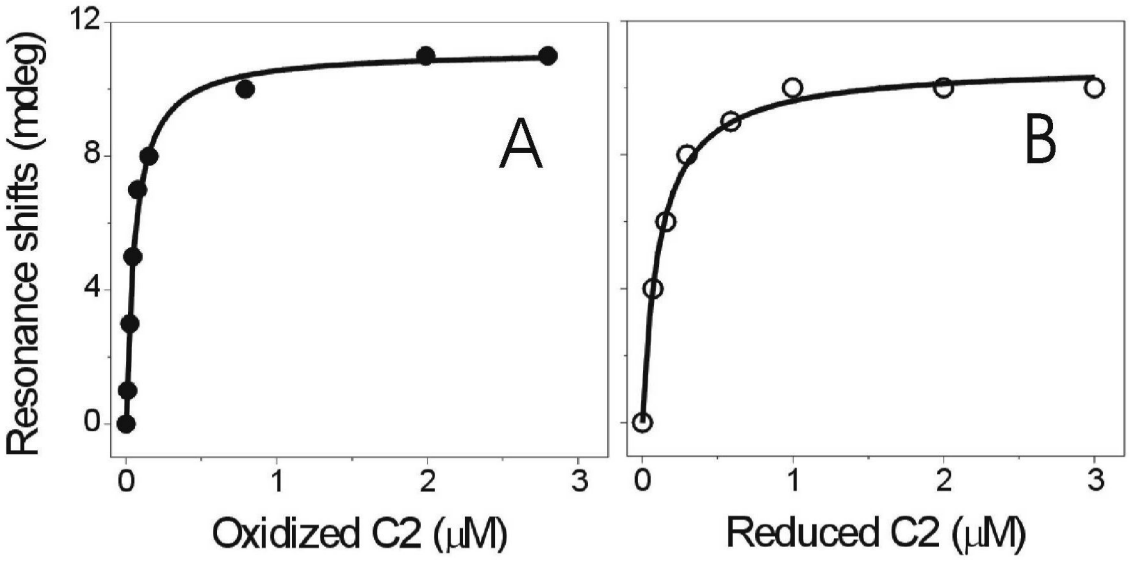

Figure 4.

Binding of C2 to oxidized bilayer-incorporated BC1 in the presence of stigmatellin. A. Titration of oxidized BC1 with oxidized C2, shown only for p-polarized data, solid line, fit with a single hyperbolic curve. Titration of oxidized BC1 with reduced C2, solid line, fit with a single hyperbola. Conditions as in Figure 1.

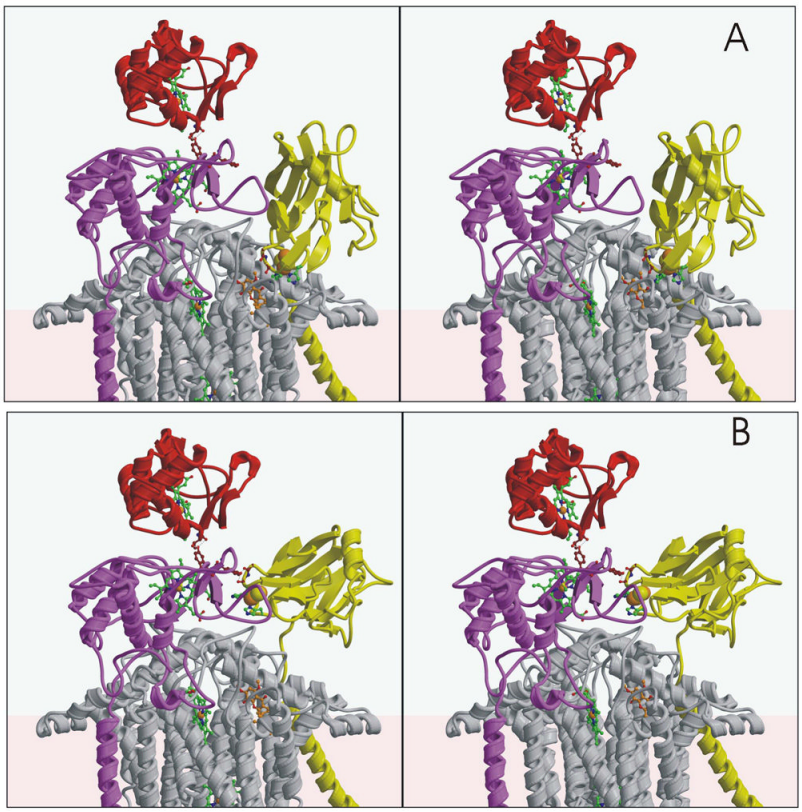

Figure 5.
Ribbon structure of hypothetical C1/C2/Rieske protein complexes. Red C2, yellow ISP, maroon C1, gray B, green heme, orange stigmatellin, and yellow and brown spheres the iron-sulfur cluster. C1 Y152 and Y153 side chains and amino acids that appear to interact with C1 (ISP – P154 and H156, C2 – T15) are brown A. Structure in the presence of stigmatellin, with the Rieske iron-sulfur cluster close to B ("B" position). B. Structure in the absence of stigmatellin, with the Rieske iron-sulfur cluster near C1 ("C1" position). Stigmatellin is shown in both structures as a marker of the Qo site.

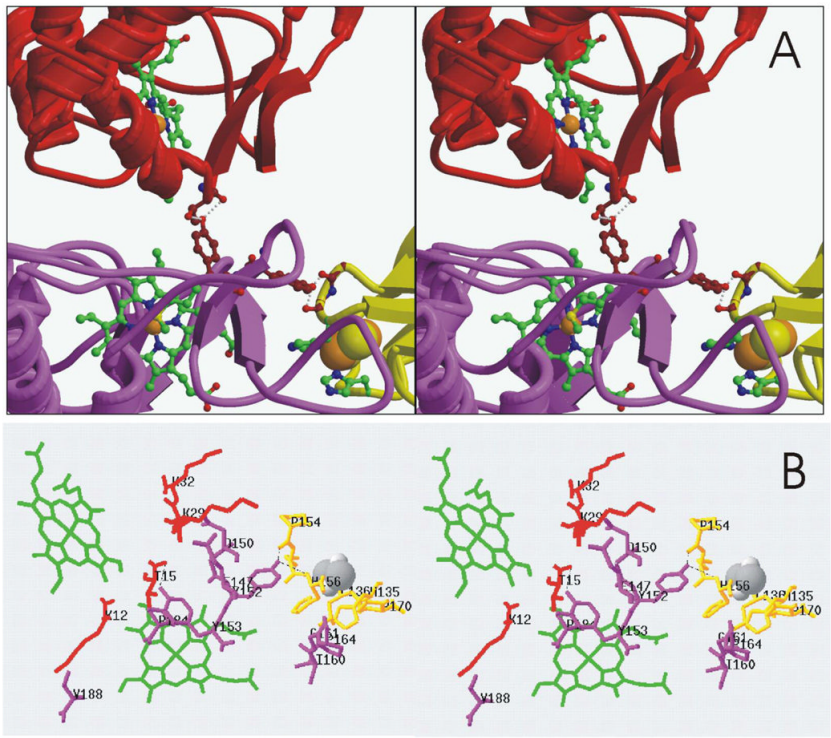

Figure 6.

Stereo views of the C1/C2/ISP interaction domains. A. Ribbon representation with the hemes, stigmatellin, and tyrosine 152 and 153 as ball and stick (Detail enlarged from Figure 5b). Y153 is in the center and Y152 left of center. B. Ball and stick representation of the C1-ISP and C2-C1 interactions domains. Shown are amino acids which are within 3.5 Å of C1, C1 - maroon (E147, D150, Y152, Y153, I160, G161, P164, P184, V188), C2 - red (K12, T15, K29, G30, A31, K32), ISP - gold (H135, I136, P154, C155, H156, P170) , ISP iron-sulfur cluster – gray, and hemes – green (C2 heme, upper left). Hydrogen bonds are shown as dashed lines and include C1-Y153 to C2 – T15, and C1-Y152 to P154 and H156 backbone atoms).

Table 1

K_D values for the interaction of *Rb. capsulatus* C2 and BC1.

	K_D(μM)[1] BC1/C2 Redox State[2]		
C2	**Oxidized/Oxidized**	**Oxidized/Reduced**	**Reduced/Reduced**
WT[3]	0.110 ± 0.010↑ 0.58 ± 0.01↓	3.1 ± 0.3↓	0.020 ± 0.003↑
K93P	0.050 ± 0.002↑ 0.63 ± 0.02↓	ND[4]	0.023 ± 0.002↑
WT + stigmatellin	0.06 ± 0.01↑	0.11 ± 0.01↑	ND

[1] K_D values are the average of those determined for the *p*- and *s*-polarization fits.

[2] Arrows indicate a decrease(↓) or increase (↑) in total mass density.

[3] WT = wild-type

[4] ND = not determined